Journal of Directed Energy, **4**, Winter 2010, 147–167

A System Engineering Approach for Active Track Jitter Performance Evaluation

J. Negro*

[1]*Boeing-SVS, Inc., 4411 the 25th Way, Suite 350, Albuquerque, New Mexico 87109*

R. Brunson

2209 Garden Rd NE, Rio Rancho, NM 87124

D. Dean

Boeing-SVS, Inc., 4411 the 25th Way, Suite 350, Albuquerque, New Mexico 87109

J. Kann

Boeing-LTS, Kirtland Air Force Base, New Mexico 87117

and

E. Duff

Air Force Research Laboratory/RDTP, Kirtland Air Force Base, New Mexico 87117

This paper describes an engineering error budget approach for examining the design and jitter performance of active track systems used for imaging and high-energy laser beam control applications. This root-sum-square approach aggregates numerous design parameters into key performance variables that capture in a simplified way the engagement, environment, and essential design characteristics of an active track system. The study emphasizes the line-of-sight jitter performance of the active track system operating in turbulent media. Major error components are described for tracker measurement noise, residual atmospheric tilt turbulence, residual local optical system tilt jitter, jitter coupling error, and active signature errors (including speckle and scintillation). Algebraic models for each of these terms are derived from analytic models, simulations, or empirical experience. These models are combined into an overall system engineering model error budget. The model is exercised for a generic ground-to-space imaging application to illustrate the methodology. This active track model segregates error terms unique to active track and shows the jitter performance penalty of active track systems in comparison to comparable passive systems.

KEYWORDS:
Active track, Jitter, Track performance

Received October 21, 2010.
*Corresponding author; e-mail: James.e.negro@boeing.com.

Nomenclature

C_n^2	atmospheric refraction structure function
D_I	diameter of illuminator at target (FWHM) in angle units (μrad)
D_{PSF}	size of point spread function at tracker focal plane array in units of output space angle (μrad)
D_R	diameter of receiver (circular aperture assumed)
D_T	diameter of target in angle units (μrad)
D_{XMTR}	diameter of illuminator beam projecting (transmitting) aperture
f_{BW}	receiver servo control track loop bandwidth (zero-gain cross-over; see also $f_{3\text{dB}}$)
f_d	local disturbance jitter spectra bandwidth parameter
f_s	sensor sample rate
f_{TG}	Tyler frequency characterizing spectra of atmospheric turbulence tilt component (Hz)
$f_{3\text{dB}}$	track servo control bandwidth frequency (Hz) (closed loop gain down 3 dB; see also f_{BW})
$G_{\text{rej}}(f)$	disturbance error rejection function
h	altitude parameter
h_x, h_y	target size dimensions (rectangular targets)
IFOV	tracker detector array pixel field-of-view (μrad)
K_A	aperture factor
K_d	local disturbance jitter spectra normalization parameter
N_B	number of independent beamlets in a multibeam illuminator (dimensionless)
n	adaptive optics array dimension ($n \times n$)
n_{Bkgnd}	background noise
n_e	detector noise (dark current, readout)
n_T	nondimensionalized target diameter (multiples of λ/D)
P_R	received LADAR power
P_T	transmitted LADAR power
q_E	detector quantum efficiency
R	range (distance between LADAR and target)
Rytov	Rytov parameter (scintillation)
r_0	Fried atmospheric turbulence coherence length parameter (cm)
S	receiver signal
SNR	tracker detector signal-to-noise ratio (dimensionless)
T_F	track filter function (dimensionless)
v	apparent transverse velocity
η_{ATM}	atmospheric transmission (2-way)
η_{SYS}	optical system transmission
λ	illuminator wavelength (μm)
ξ	normalized path length parameter
σ	LADAR optical cross section of target
σ_{AS}	net residual line-of-sight (LOS) error due to active signature effects; include speckle of a coherent illuminator on an extended target with surface roughness and due to scintillation of the illuminator beam because of atmospheric turbulence

σ_{Atm}	net residual LOS error due to atmospheric turbulence induced tilt error; includes the filtering effects of the track loop bandwidth
σ_J	net active track LOS jitter composed of all error contributors
σ_{JC}	net residual LOS error due to jitter coupling of the illuminator beam on the target
σ_{JD}	net residual LOS error due to local jitter disturbances including optical alignment error and telescope jitter; includes the filtering effects of the track loop bandwidth
σ_{MJ}	local disturbance total jitter parameter
σ_{Spk}	residual LOS jitter due to speckle
σ_{Sct}	residual LOS jitter due to scintillation
σ_T	net transmitted illuminator beam jitter
σ_{Trk}	net residual LOS error due to tracker measurement error; includes the effects of sensor SNR, turbulence effects on the optical point spread function, and the filtering effects of the track loop bandwidth
σ_{θ_G}	G-tilt jitter due to atmospheric turbulence
σ_{θ_S}	speckle jitter (total)
$\Phi_{\text{dd}}(f)$	local jitter disturbance spectra
χ_i	track error measurement noise "chi" degradation factors
χ_{JC}	jitter coupling chi factor
ψ	nadir angle (complement of elevation angle)

1. Introduction

Ever since lasers were developed, their use as very accurate laser detection and ranging systems (LADAR) have been envisioned to make use of their accuracy advantage, in comparison to radio frequency (RF) radars, due to their much shorter wavelength. Indeed LADAR are similar enough to radars that the same performance equations can be applied. For example, the received power is given by[7]

$$P_R = \frac{P_T \sigma D_R^4 \eta_{\text{ATM}} \eta_{\text{SYS}}}{16 R^4 \lambda^2 K_A^2} \tag{1}$$

where P_R is the received signal power; P_T is the transmitter power; σ is the target cross section; D_R is the receiver aperture diameter; η_{ATM} and η_{SYS} are transmission factors for the atmosphere and system, respectively; R is the target range, λ is the wavelength; and K_A is an aperture factor. This formula allows ready calculation of the received power, which, along with the receiver detection and noise properties, allows calculation of numerous LADAR performance parameters, including maximum useful range.

This equation is a simplification, yet it allows useful initial system engineering calculations to be made in describing a LADAR system. We seek similar relationships for the line-of-sight (LOS) jitter performance of laser active tracking systems.

Laser active tracking systems are useful in situations in which the tracked object's passive thermal or solar illumination signatures are inadequate for accurate tracking. We note that for modest illuminator powers, the in-band solar illumination is on a par with, or greater than, that of the LADAR illuminator. Therefore, LADAR systems are most useful

in situations in which accurate range/Doppler measurements are needed, or in which there is no solar illumination.

The primary objective of this work has been to develop a performance model of the LOS performance of an active track system suitable for system architectural trades, top-level system engineering performance evaluations, and top-level design trades. To be useful at the system engineering level, the model should not include detailed design parameters, nor should it rely on the use of complex computer codes and simulations. These LOS performance tools are intended only for top-level trades. The detailed design tools are required for system design. Although simple models are desired, often the complexities of atmospheric turbulence and local jitter, for example, will require scenario- and application specific calculations. These may appear to violate our desire to keep things simple, but these more complex calculations can be done once per system analysis, thus still allowing a meaningful system engineering trade.

One of the issues in past system trades is that active track systems have been baselined as preferable to passive systems for 24-h scenarios and then did not deliver the performance they initially promised. Therefore, another objective of this study is to realistically include the effects of active track system performance degraders. This would allow system architects to make realistic trades in which active track systems provide but one choice, whereas passive track systems may provide reasonable alternative choices. It would also allow technologists to better determine the performance drivers in implementing active track systems.

In summary, the active track LOS performance models should do the following:

- Capture key salient features of active track system performance
  - deleterious effects of atmospheric turbulence
  - imperfect adaptive optics systems
  - target signature characteristics (speckle, scintillation)
  - local disturbance jitter
  - temporal effects of control system bandwidth
- Where possible, segregate active and passive track effects
- Be computationally simple and easy to use
  - useful for initial performance trades and active versus passive tracking trades
  - show major performance drivers
  - show basic trends
  - suggest baseline systems for comparative evaluation with more accurate tools

A brief description of an active tracking system is presented, followed by a description of the active track system engineering LOS performance model.

The laser active tracking system entails a laser illuminator and a receiver with their associated beam control subsystems. Characteristics of the atmospheric transmission path and the target tracked object are also important for determining the overall jitter performance of the system. These key subsystems are illustrated in Fig. 1. This figure shall be used to identify the key parameters describing the system and its performance. The acquisition sensor, the passive sensor, and the inertial reference are used for support functions. The other subsystems (with gray arrows) directly affect active track performance.

The laser illuminator source is an essential element in an active track system. The total power and optical quality of the beam directly affect the illuminator irradiance on target. Here optical quality is meant to include the inherent beam quality of the laser device and

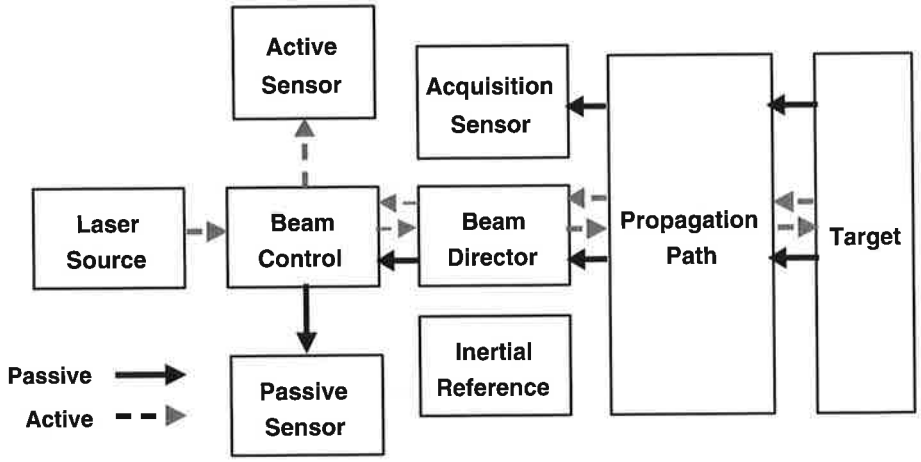

Fig. 1. Functional block diagram of an active track system illustrating the key subsystems.

the wavefront quality of the optics from the device up to and including the illuminator projecting telescope. In this analysis, all these effects are represented by the far-field beam size parameter D_I. The laser wavelength and coherence affect the illuminator interaction with the target in producing a return signal to the receiver and determine, with the receiver aperture size, the "diffraction" limit of the system. The return signal is also impacted by the coherence of the illuminator and the number of beamlets used to form the beam, as well as the far-field beam irradiance pattern.

The active sensor includes the detector array and track algorithms that calculate measured LOS error at each sensor sample from the detector pixel array readouts. Important sensor characteristics include the pixel instantaneous field of view (IFOV), the detector quantum efficiency (q_E), the sensor and background noise (n_e, n_{Bkgnd}), and the sensor integration time and sample rate (f_S).

Beam control and beam director subsystems are used to accurately direct the illuminator beam toward the target. Usually, a smaller aperture is used for the illuminator pointing system to broaden the beam to cover the target. In most cases, the aperture is separate from the receiver aperture, though the apertures may be spatially shared. Important parameters are the net transmitted illuminator beam jitter (σ_T) and the effective aperture diameter (D_{XMTR}). The servo control bandwidth (f_{BW}) and the effective receiver aperture diameter (D_R) are important parameters for the receiver beam control system.

The propagation path is important as it includes the target range (R) and, in many cases, atmospheric turbulence. The turbulence can distort both the illuminator beam and received signal intensity patterns. The tilt component is a jitter disturbance. These effects are represented by the standard atmospheric turbulence characterization parameters: the Fried coherence length (r_0), the Rytov parameter (Rytov), and the Tyler frequency (f_{TG}). Of course, these terms implicitly incorporate other terms such as the atmospheric structure function C_n^2, the apparent winds, including LOS slew rate, and aperture size (D).

Finally, the target optical cross section, reflectance map, size, and "detail" are all qualities that impact the signal level and information that might be detected by the track sensor.

Table 1. Definition of active track error contributors

Jitter Term	Description
σ_J	Net active track LOS jitter composed of all error contributors.
σ_{Trk}	Net residual LOS error due to tracker measurement error. This includes the effects of sensor SNR, turbulence effects on the optical point spread function, and the filtering effects of the track loop bandwidth.
σ_{Atm}	Net residual LOS error due to atmospheric turbulence induced tilt error. This includes the filtering effects of the track loop bandwidth.
σ_{JD}	Net residual LOS error due to local jitter disturbances including optical alignment error and telescope jitter. This includes the filtering effects of the track loop bandwidth.
σ_{JC}	Net residual LOS error due to jitter coupling of the illuminator beam on the target.
σ_{AS}	Net residual LOS error due to active signature effects. These include speckle of a coherent illuminator on an extended target with surface roughness and due to scintillation of the illuminator beam because of atmospheric turbulence.

2. System Engineering LOS Performance Model Development

Initial approaches to this problem attempted to use a simple λ/D scaling formula with degradation factors to account for off-nominal or less-optimal-than-desired design values. This approach suffered from not utilizing the true RSS nature of independent error sources and not adequately distinguishing active track from corresponding passive track cases. Recognizing that errors due to residual atmospheric tilt and local disturbance jitter were common to both active and passive track systems led to the following system engineering error formula:

$$\sigma_J = \left[\sigma_{\text{Trk}}^2 + \sigma_{\text{Atm}}^2 + \sigma_{\text{JD}}^2 + \sigma_{\text{JC}}^2 + \sigma_{\text{AS}}^2\right]^{1/2}. \tag{2}$$

Each of the terms in this jitter equation represents a major error source. Table 1 defines these LOS jitter contributors. Model development for each of these terms then follows.

For many applications, the track noise σ_{Trk} is the dominant contributor to overall LOS jitter. It is also the most complicated. We shall find in the following that degradation factors are a suitable way to handle some of the contributors to σ_{Trk}, although this approach is not unique. The jitter formulation of Eq. (2) segregates the active track unique terms σ_{JC} and σ_{AS}. The first term is due to jitter coupling, and the second term addresses active track target signature issues of speckle and scintillation. Although the track noise σ_{Trk} might depend on active track parameters [e.g., signal-to-noise ratio (SNR)], these are not unique to active track systems,[†] and the resulting performance will be similar, at least in cases in which sufficient SNR exists to support passive track. Furthermore, the terms σ_{Atm} and σ_{JD} due to

[†]This is because the performance of passive systems depends in a similar way on SNR, even though the basis for SNR calculation is much different for passive systems.

atmospheric turbulence tilt and local disturbance jitter, respectively, apply equally to active and passive track cases provided that any wavelength differences are taken into account.

2.1. Track Sensor Jitter

Track sensor jitter depends on numerous factors. The fundamental error mechanism occurs in the process of calculating LOS motion from the detector array pixel data processed with a specific track algorithm. Numerous complications occur in this process and impact the measured track error. The complications include detector noise, which is modeled here, and numerous other effects, which are not explicitly modeled here but must be taken into account in a track sensor design.[‡] Furthermore, the tracker measurements are in a real sense filtered by the track servo control of the LOS so that the servo control track function (typically) reduces the sample-to-sample measurement noise of the track sensor. The low-frequency measurement noise becomes jitter, because the track control loop follows this low-frequency input, but the high-frequency components are too high in frequency to be followed by the low-frequency track loop. Typically, the noise of a tracker is modeled to be independent from sample to sample because the detector and signal shot noise are statistically independent sample to sample.

A fundamental noise source is the detector noise associated with each detector array pixel output. Fundamentally these noise sources include shot noise, background noise, and detector read noise. These noise sources combine with the overall signal level S to determine the shot noise and, with the other noise sources, the SNR as shown in the equation

$$\mathrm{SNR} = \frac{S}{\sqrt{S + n_e^2 + n_{\mathrm{Bkgnd}}^2}}, \tag{3}$$

where S is the signal level, n_e is the detector noise, and n_{Bkgnd} is the background noise. S itself depends on numerous factors including, but not limited to, illuminator power and beam quality, illuminator spot size at the target, path transmission, target reflectivity, and detector quantum efficiency. Path transmission includes transmission through the optical systems as well as atmospheric transmission.

It is important to note that the use of a single SNR parameter "aggregates" these many more detailed system parameters.

The track performance is determined fundamentally by the classic quad cell equation

$$\sigma_{\mathrm{Tkr}} \propto \frac{1}{\mathrm{SNR}} \cdot \frac{\lambda}{D_R}, \tag{4}$$

Note that the jitter equation [Eq. (4)] includes the ratio λ / D_R representing the diffraction-limited spot size of the receiver optical system, where λ is the illuminator wavelength and D_R is the receiver aperture.

For this work we use the more complete version due to Tyler and Fried for a quad cell sensor array which takes into account target size[10]:

$$\sigma_{\mathrm{Tkr}} = \frac{\pi \left[(3/16)^2 + (n_T/8)^2\right]^{1/2}}{\mathrm{SNR}} \left(\frac{\lambda}{D_R}\right). \tag{5}$$

[‡]There are numerous track sensor error contributors, including response uniformity, readout quantization, and data latency.

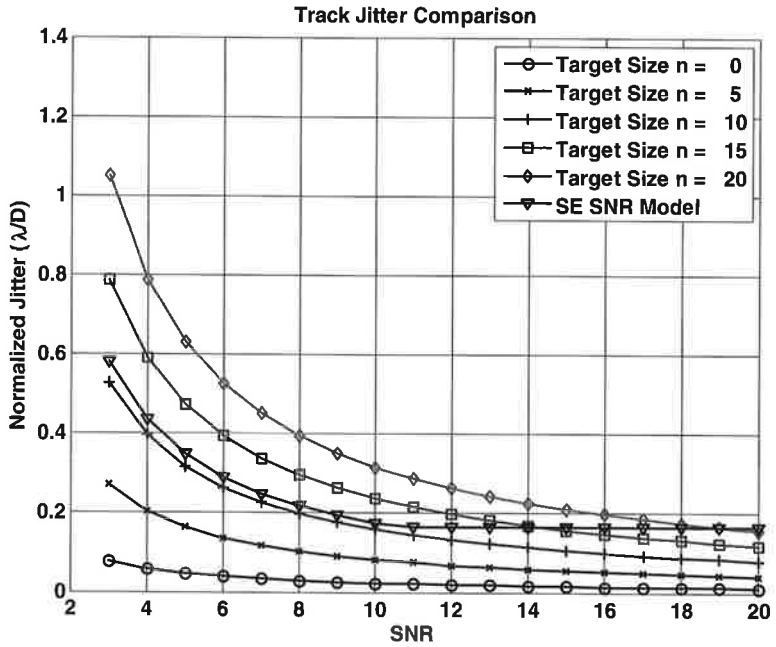

Fig. 2. Comparison of track noise models. (In the legend, target size "n" is the normalized target size "n_T" in the text.)

The parameter n_T represents the normalized target size[§]. This equation is modified for the present analysis to account for the servo control track filter effect T_F limiting the fraction of tracker noise that actually ends up as true LOS jitter and to account for system imperfections that degrade performance by use of χ_i factors, as explained below. This gives

$$\sigma_{\mathrm{Tkr}} = \left(\prod_i \chi_i\right) \cdot T_F \frac{\pi\left[(3/16)^2 + (n_T/8)^2\right]^{1/2}}{\mathrm{SNR}} \left(\frac{\lambda}{D_R}\right) \tag{6}$$

The degradation factors can represent effects due to impacts either on the effective SNR or on the effective resolution (λ/D). Non-diffraction-limited optical performance can be represented by effectively increasing this ratio through the use of an appropriate χ degradation factor. The effects of atmospheric turbulence in limiting the diffraction-limited performance are explicitly handled with a χ degradation factor.

Equation (6) is plotted in Fig. 2 along with the SE SNR degradation factor formulation [Eq. (7)] with a minimum χ_{SNR} of 2/3. These plots show that the empirical degradation model is a good fit for target sizes corresponding to $n_T \sim 11$. Because the Tyler–Fried model captures noise variations with target size, this is the preferred model to be used in

[§]n_T is taken to be the largest target dimension in units of diffraction spot size. Thus, the angular size of the target is given as $n_T{}^*\lambda/D$.

Table 2. Degradation factor table for tracker noise

Degradation factor	Effect	Comments
χ_1	AO turbulence higher order effects	Primarily addresses the increase in the image plane point-spread function due to atmospheric turbulence and the inability of the adaptive optics system to correct it.
χ_2	Focal plane sampling – pixel resolution	Primarily addresses whether the image is Nyquist sampled.
χ_3	Target characteristics and track algorithm	The factor is intended to capture difference between point and extended image targets, the characteristics (detail) of extended image targets, and relationship of these target characteristics to the track algorithm.
χ_4	(Reserved)	

this performance model:

$$\text{SE Model} : \sigma_{\text{Tkr}} = \left(\prod_{i=1}^{3} \chi_i \right) 0.3 \chi_{\text{SNR}} \left(\frac{\lambda}{D_R} \right), \tag{7}$$

where

$$\chi_{\text{SNR}} = \max \left(\frac{7}{\text{SNR}}, \frac{2}{3} \right) \tag{8}$$

and the χ_i are as described below. Values of 1.0 are used for the plot.

The $n_T = 0$ case corresponds to a point source target. Note from the figure the large track noise performance penalty for large extended targets. This is an important effect to take into account when designing track systems. This effect occurs for passive as well as active track systems[¶] . These effects are included in the χ_3 parameter, described below.

Table 2 gives three degradation factors for track noise. It shows degradation factors for AO turbulence effects, focal plane (under)sampling, and target characteristics (and track algorithm selection). This section details the derivation of each of these degradation factors.

2.1.1. Track Noise Degradation Factor for AO Turbulence Effects. This degradation factor is intended to model the deleterious effects of atmospheric turbulence and the limited capability of an adaptive optics system to correct it. The key modeled effect is turbulent smearing of the optical system point spread function and a reduction in the point spread function main lobe signal power. Temporal effects are not addressed; the AO system is

[¶]Note that the Tyler–Fried result pertains to a centroid tracker. Performance variations due to an advanced tracker (i.e., correlation) can be handled via an appropriate χ factor.

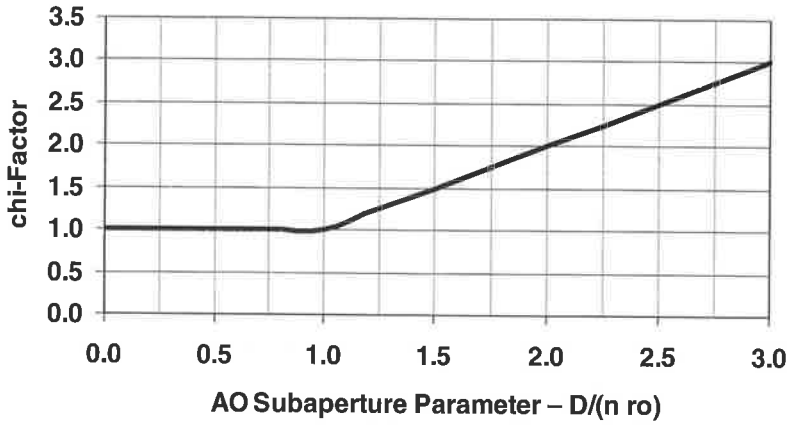

Fig. 3. χ-Factor for AO design (less than full number of subapertures).

assumed to have adequate bandwidth. Rather, the emphasis is on the spatial resolution when using an AO system. Degradation occurs when the AO system has an inadequate number of subapertures (resolution) as well as insufficient temporal bandwidth:

$$\chi_1 = \max\left(1, \frac{D}{n \cdot r_0}\right). \tag{9}$$

The key effect modeled here is the residual effect of atmospheric turbulence in smearing the target image and in degrading the optical quality of the track system to something less than diffraction limited. The AO degradation term, plotted in Fig. 3, primarily addresses the case when the aperture is significantly larger than the Fried parameter and there are an inadequate number of AO subapertures (sensor, actuator, or both) to correct these aberrations. The residual aberrations effectively increase the size of the optical system point spread function, thereby decreasing the track resolution and sensitivity. They also reduces the fraction of energy in the main diffraction lobe. Typically, the adaptive optics errors are higher order Zernike terms. For that reason, the diffraction main central lobe can have nearly the same width as a diffraction-limited system, but the overall point spread function has a large "halo" surrounding the main lobe. The halo degrades tracking performance.

2.1.2. Track Noise Degradation Factor for Focal Plane (Under)Sampling. This degradation factor models the effects of focal plane image sampling by the detector array. Typically "Nyquist" sampling of two or more pixels per PSF is preferred. However, if the image is oversampled, the signal per pixel is reduced. If the image is undersampled, the resolution of the optical system is not utilized:

$$\chi_2 = \max\left(\frac{1}{10} \cdot \frac{2 \cdot \text{IFOV}}{D_{\text{PSF}}}, 1\right). \tag{10}$$

Note that this degradation factor, plotted in Fig. 4, is linear in the ratio IFOV/D_{PSF}. Note that this term addresses only the focal plane sampling as the diffraction is directly captured in the λ/D term of the track error equation. Note that in the original work, this term had a greater sensitivity, but once it was realized that the larger pixel size had only a small impact on track noise, the sensitivity was reduced $10\times$. This factor can be eliminated with little loss.

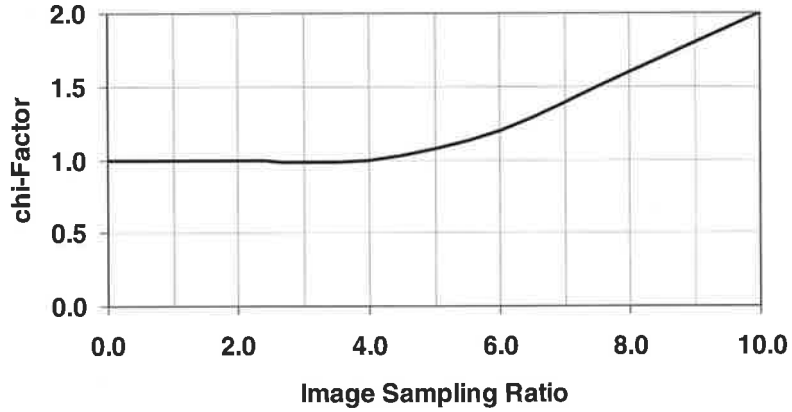

Fig. 4. χ-Factor for focal plane sampling ratio (0.2 IFOV/D_{PSF}).

2.1.3. Track Algorithms and Noise Degradation Factor Target Characteristics. Targets are generally of two types—resolved and unresolved with respect to the tracker resolution. Unresolved targets appear essentially as point sources and are reasonably tracked by quad cell–type trackers. These targets are insensitive to scintillation and speckle and, to a lesser extent, less sensitive to jitter coupling. Resolved targets are also referred to as "extended" targets. Details of the target geometry and variations in its surface spatial distribution can be observed. This spatial detail offers attractive advantages for more complex track algorithms, such as correlation track, but makes the tracker more susceptible to error mechanisms including target aspect variations, glint, speckle, scintillation, and jitter coupling.

A variety of track algorithms can be used for extended resolved targets. These algorithms include centroid, binary centroid, edge, and correlation track algorithms. Modern algorithmic approaches include Bayesian and active contour tracking (ACT).

Oblong targets such as missiles present special challenges to the tracker because only a few edge pixels contribute to the measurement of track error along the long body axis. These considerations have led to special algorithms such as the 19-point track algorithm.

There is no definitive description of the variation in track performance with target characteristics and track algorithm. The values used in this analysis are somewhat notional. Better performance estimates need to be determined with analysis and simulations for specific application cases, once these are defined. It is clear that target signature effects such as jitter coupling, speckle, and scintillation will also depend on the details of the track algorithms. These relationships are not well understood in a general context. They need to be investigated in detail as an active track system technology matures:

$$\chi_3 \begin{cases} 1.05 & \text{point target (unresolved); centroid tracker} \\ 1.00 & \text{missile target (transverse axis); centroid tracker} \\ 2.00 & \text{missile target (longitudinal axis); 19-point edge tracker} \\ 1.00 & \text{extended target (resolved); correlation, Bayesian or ACT tracker,} \end{cases} \tag{11}$$

Unlike the previous degradation factors, the target type is a discrete variable degrader. Four classes of targets are considered. The first is an unresolved point target. The second and third are for missile body–type targets for which there is a significant difference between longitudinal and transverse tracking performance. The fourth target is for an extended resolved target with "good" contrast. The point source target is considered the baseline. Note the extended target case showing the counterintuitive result that correlation tracking is no better than centroid tracking for an extended target. These simplifications are based on the experiences of many practitioners.

Recall that the overall performance equation is composed of five terms, as shown here:

$$\sigma_J = \left[\sigma_{\text{Trk}}^2 + \sigma_{\text{Atm}}^2 + \sigma_{\text{JD}}^2 + \sigma_{\text{JC}}^2 + \sigma_{\text{AS}}^2\right]^{1/2} \tag{12}$$

The discussion to this point has emphasized the first term. The remaining terms are now addressed.

2.2. Atmospheric turbulence jitter‖ σ_{Atm}

The presence of atmospheric turbulence introduces dynamic tilt between the optical system and its target. Standard atmospheric turbulence theory (e.g., Refs. 2 and 3) quantifies the total per-axis tilt contributed by the atmospheric turbulence as a function of the Fried parameter r_0 and the receiver aperture diameter. The residual tilt depends on the disturbance tilt frequency content (spectra) and the bandwidth capability of the tilt control system:

$$\sigma_{\theta G}^2 = 0.17 \cdot \left(\frac{\lambda}{D_R}\right)^2 \left(\frac{D_R}{r_0}\right)^{5/3}, \tag{13}$$

$$r_0 = 0.185\lambda^{6/5} (\cos\psi)^{3/5} \left[\int_0^\infty C_n^2(h)dh\right]^{-3/5}, \tag{14}$$

where $C_n{}^2$ is the atmospheric refraction structure function, h is the altitude, and ψ is the zenith angle**. Tyler and Frical[10] define a characteristic tilt frequency f_{T_G} such that

$$f_{T_G} = 0.333 D_R^{-1/6} \lambda^{-1} \sec^{1/2}\psi \left[\int_0^\infty C_n^2(h) v^2(h) dh\right]^{1/2}, \tag{15}$$

where $v(h)$ is the apparent wind due to both true wind and the effect of an angular slew of the LOS. Given these relationships, an expression for the residual atmospheric turbulence–induced LOS tilt error is

$$\sigma_{\text{Atm}}^2 = \left(\frac{f_{T_G}}{f_{3\text{dB}}}\right)^2 \cdot \left(\frac{\lambda}{D_R}\right)^2, \tag{16}$$

where $f_{3\text{dB}}$ is the tracker control bandwidth††.

‖Note that this section address residual atmospheric turbulence tilt error. Higher order aberrations impact the optical spot spread function, and their effects on track error are represented through a degradation factor on track noise.

**That is, the complement of the elevation angle: $\psi = \pi/2 - \theta_{\text{EL}}$.

††The term $f_{3\text{dB}}$ is used here to be consistent with the literature. Later, we shall use the term f_{BW} to represent the control bandwidth, defined in this case as the open loop gain crossover frequency. For simple controllers, $f_{3\text{dB}} = f_{\text{BW}}$.

In summary, the residual atmospheric turbulence–induced LOS tilt error is a complex function of atmospheric turbulence characterization parameters and the tracking system optical and control system characteristics. These errors can be estimated with the formulas provided above or with more detailed Monte Carlo wave propagation simulations. Experimental data are often plotted as a function of the Rytov parameter, which can be computed in a variety of ways.[2,3,5] We use the Rytov parameter to characterize scintillation effects in a later section of this paper:

$$\text{Rytov} = 0.5631\left(\frac{2\pi}{\lambda}\right)^{7/6} R^{11/6}\int_0^1 d\xi C_n^2\left[h\left(R\xi\right)\right]\left[\xi\left(1-\xi\right)\right]^{5/6} \tag{17}$$

2.3. Local jitter disturbances σ_{JD}

The effects of local mechanical vibration and local path jitter residual disturbances are best represented through the disturbance power spectral density and the error rejection function of the track control system. We take here the disturbance to be the net optical jitter disturbance presented to the track loop. Defined in this way, the effects of internal alignment and stabilization loops, if any, have already been taken into account:

$$\sigma_{\text{JD}} = \left[\int_0^\infty \Phi_{\text{dd}}(f)\left|G_{\text{rej}}(f)\right|^2 df\right]^{1/2}. \tag{18}$$

The details of the terms $\Phi_{\text{dd}}(f)$ and $G_{\text{rej}}(f)$ are specific to each application. One example case is illustrated here. The methodology can be followed with more detailed models for the application being investigated. We assume that the disturbance is given by

$$\Phi_{\text{dd}}(f) = \frac{K_d}{1+\left(f/f_d\right)^2} \tag{19}$$

representing a first-order Markov process, where

$$K_d = \frac{2}{\pi f_d}\sigma_{\text{MJ}}^2 \tag{20}$$

with σ_{MJ}^2 representing the net disturbance variance and f_d the characteristic frequency of the process. The disturbance rejection transfer function of the track loop controller is

$$\left|G_{\text{rej}}(f)\right|^2 = \frac{f^2}{f^2+f_{\text{BW}}^2} \tag{21}$$

corresponding to a first order Type I control system.

With these models, it is not too difficult to show that

$$\sigma_{\text{JD}} = \sigma_{\text{MJ}}\left[\frac{f_d}{f_d+f_{\text{BW}}}\right]^{1/2}, \tag{22}$$

which has asymptotic limits

$$\sigma_{\text{JD}} = \begin{cases} \sigma_{\text{MJ}};\ f_{\text{BW}} = 0 \\ \text{and} \\ \sigma_{\text{MJ}}\cdot\left(\dfrac{f_d}{f_{\text{BW}}}\right)^{1/2} \quad \text{for} \quad f_{\text{BW}} \gg f_d \end{cases}. \tag{23}$$

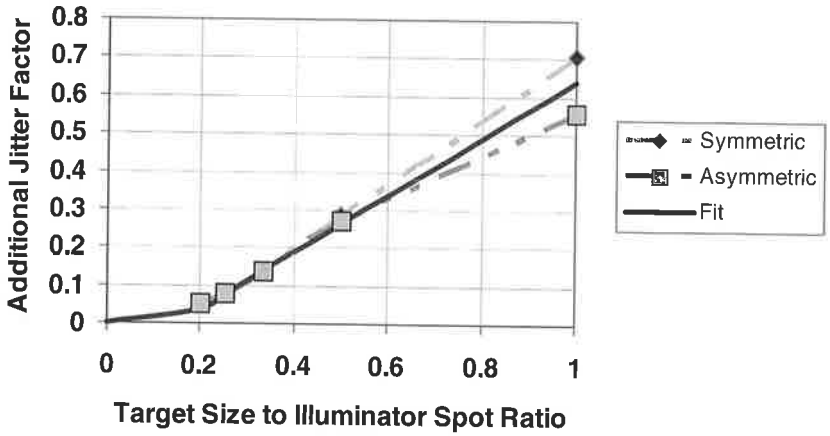

Fig. 5. Coupling error for illuminator spot size to target size ratios.

Of course, the precise details of these relationships depend on the assumed spectra for the disturbance and the servo control design. Nonetheless, the key features are that the residual disturbance is a function of the disturbance RMS jitter (σ_{MJ}), the disturbance bandwidth (f_d), and the servo control bandwidth (f_{BW}).

2.4. Jitter coupling σ_{JC}

In active track, an illuminator beam shines on the target and its reflection to a receiver is the target signature sensed by the tracker focal plane and processed to determine track error. Jitter of a nonuniform illuminator beam itself modulates the illumination of the target and causes a portion of the illuminator jitter to be sensed as apparent target motion and, hence, tracking jitter. This phenomenon has been observed in practice and analyzed.[††] Dr. Jim Riker of the U.S. Air Force developed a simple analytic model for a flat plate that illustrates how a fraction of a Gaussian illuminator beam pattern jitter couples into the sensed target jitter. The fraction of coupling depends primarily on the relative size of the Gaussian illuminator beam pattern with respect to the target size. Coupling ratios of 20%–100% can be realized for illuminator-to-target-size ratios (linear dimension) of 1–5.

This analysis is based on Riker's work in which he analytically, and with simulations, investigated the centroid track errors for rectangular flat plat targets. He explored variations in target aspect (height-to-width ratio), illuminator-beam-to-target-size ratio, and illuminator jitter. To minimize jitter coupling, the illuminator far-field beam size needs to be large relative to the target. But this will mean that the illuminator beam energy is not used very efficiently and the signal level will decrease. His key result, described in an Air Force technical memorandum and Refs. 4 and 8, is plotted in Fig. 5. Here the results are plotted as a function of the target-diameter-to-illuminator-spot-diameter ratio (D_T/D_I) rather than the inverse ratio (i.e., D_I/D_T) Riker uses. Note that the result is nearly linear in this form

[††]Unpublished AFRL internal Technical Memoranda.

and leads to the following mathematical representation:

$$\chi_{\mathrm{JC}} = \max\left[0.75 * \left(\frac{D_T}{D_I} - 0.15\right),\ 0\right]. \tag{24}$$

Jitter coupling is only a part of the story. To determine the total LOS jitter due to this term, two additional aspects of the problem must be taken into account. First, the illuminator jitter must be estimated, because the jitter coupling coefficient simply determines the fraction of the illuminator jitter that is coupled into measured track jitter. Second, the track loop control system bandwidth must be taken into account, because only a portion of the illuminator beam jitter coupling error will result in a LOS error.

Active track systems are typically bistatic. The transmit aperture is distinct from the receiver aperture, even though they may both be on the same gimbal or the same optics may be spatially shared. So the pointing jitter of the transmitter will be different from the LOS jitter of the receiver optical path. For this reason, an estimate of the illuminator transmitter jitter (at the target) will be required to estimate jitter coupling.

For several reasons, we can expect the illuminator pointing jitter to be somewhat larger than the receiver jitter. The key reasons for its larger pointing error are that the illuminator subsystem has a smaller aperture and it has a lower net SNR. We assume here that the illuminator jitter is known or estimated so that this value can be used in the receiver LOS jitter coupling calculations. Calculation of the illuminator pointing jitter can initially be done using the methodology described in this paper for LOS jitter using the parameters for the smaller transmit aperture illuminator pointing system.

In summary, the jitter coupling contribution to overall LOS jitter is modeled as

$$\sigma_{\mathrm{JC}} = T_F \chi_{\mathrm{JC}} \cdot \sigma_T, \tag{25}$$

where σ_T is the pointing jitter of the illuminator beam, T_F is the track loop noise transmission factor,[§§] and χ_{JC} is the jitter coupling factor. The jitter coupling factor χ_{JC} used here is a simple algebraic function of the target angular size and the illuminator beam spot size, as given in Eq. (24). Typically illuminator-to-target-size ratios D_I/D_T of 3–5 are expected. We do not detail the calculation of σ_T here because its form is very similar to that of σ_J. Generally we expect $\sigma_T > \sigma_J$ because the transmit aperture is 3–10× smaller than the receiver aperture. A major portion of illuminator pointing jitter will be uncorrelated with the receiver atmospheric jitter so that jitter coupling error can be RSS'd with the other error terms.

2.5. Active signature (speckle and scintillation) σ_{AS}

The active track target signature has two additional effects not present in passive track.[¶¶] Those effects are scintillation and speckle. Scintillation is a non-Gaussian and rapidly changing far-field illuminator beam pattern due to the effects of atmospheric turbulence. Speckle is the effect of interference of the illuminator beam hitting parts of the target

[§§] T_f values of 0.2–0.5 are typical.

[¶¶] Scintillation can occur in passive systems, but in a way different from that explained above for active systems. In passive systems, the *received* signal scintillates. This is quite distinct from the illuminator scintillation at the target.

at different depths that are within one receiver resolution distance of one another. In the following, RMS jitter error equations for the speckle (σ_{Spk}) and scintillation (σ_{Sct}) are developed and combined in a straightforward RSS fashion to obtain the RMS LOS jitter due to active signature effects:

$$\sigma_{\mathrm{AS}} = \left[\sigma_{\mathrm{Spk}}^2 + \sigma_{\mathrm{Sct}}^2\right]. \tag{26}$$

2.5.1. Speckle. The speckle analysis here is based on an unpublished technical note by Lawrence Sher, of the U. S. Air Force, which, in turn, is based on the work of Baribeau and Rioux.[3]

The coherent illumination of a target introduces intensity fluctuations corresponding to constructive or destructive interference within an unresolved portion of the target. For point source targets, these fluctuations lead only to amplitude fluctuations in the return signal, but the "shape" of that return remains governed by the point spread function of the optical system and causes no jitter. For extended targets, however, the apparent fluctuations vary spatially over the dimension of the target. These fluctuations are indistinguishable from target signature variations and cause track error. Sher[9] shows that the induced track error is given by

$$\sigma_{\theta_S}^2 = \frac{1}{3\pi} \cdot \left(\frac{\lambda}{D_R}\right)^2 \left[\frac{h_x}{h_y} + \frac{h_y}{h_x}\right], \tag{27}$$

where h_x and h_y are the dimensions of a rectangular target. For square targets (i.e., $h_x = h_y$) this reduces to

$$\sigma_{\theta_S}^2 = \left(0.46\frac{\lambda}{D_R}\right)^2. \tag{28}$$

This result pertains to a single illuminator beam. If instead there are N_B mutually incoherent illuminator beams, then the speckle error is reduced by averaging in the illuminator profile:

$$\sigma_{\theta_S}^2 = \frac{1}{N_B}\left(0.46\frac{\lambda}{D_R}\right)^2 \tag{29}$$

or

$$\sigma_{\theta_S} = \frac{0.46}{\sqrt{N_B}}\frac{\lambda}{D_R}. \tag{30}$$

The Sher technical note goes on to show how this error might be attenuated by the bandwidth of the track servo. These results are very generic because there is no knowledge of the speckle frequency content. We shall assume that the speckle noise is similar to the sample-to-sample track noise in that each sampled data output is statistically independent from sample to sample. With this assumption, similar to that made by Sher for the "white noise" case, the transmission factor of the track loop can be calculated.

Combining these effects gives

$$\sigma_{\mathrm{Spk}} = \mathrm{T_F} \cdot \frac{0.46}{\sqrt{N_B}}\frac{\lambda}{D_R}. \tag{31}$$

Baribeau and Rioux[3] show that there is no advantage in filtering the image directly.

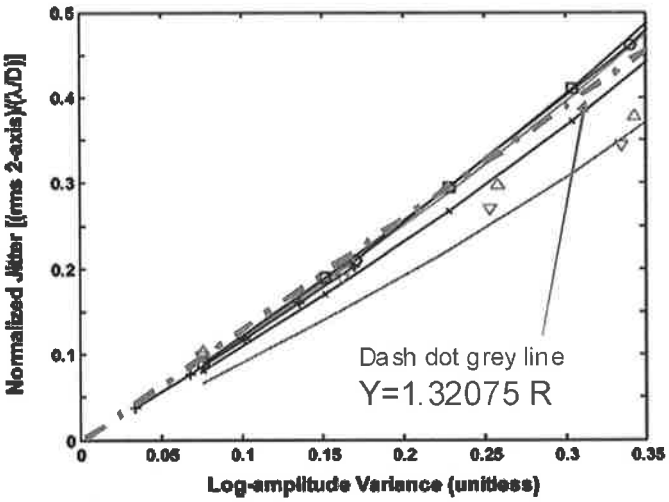

Fig. 6. Normalized jitter due to illuminator scintillation (log-amplitude variation). From Holmes[6]: Scintillation-induced jitter error (1-sigma, 2-axis, normalized by λ/D) versus spherical-wave log-amplitude variance for a 50-km path with uniform turbulence strength. Specific results include 1.06-μm wavelength, 2-m diameter aperture (solid curve with squares); 1.06 μm, 1 m (solid red curve, no symbol); 1.06 μm, 0.5 m (solid curve, crosses); 1.06 μm, 0.25 m (dotted curve, no symbol); 0.532 μm, 0.5 m (solid curve, circles); 2.12 μm, 0.5 m (solid curve, plusses); wave-optics simulation with 1.06 μm and 1 m, seed 1 (up-pointing triangles); wave-optics simulation with 1.06 μm and 1 m, seed 2 (down-pointing triangles).

Note that this speckle model assumes a relatively long-coherence-length illuminator. Speckle effects can be reduced with shorter coherence lengths.

2.5.2. Scintillation. Scintillation effects on centroid target tracking for active track illumination are addressed in the paper by Holmes.[6] He examines one case for a 50-km horizontal path of uniform turbulence and shows that the scintillation-induced jitter is relatively insensitive to aperture diameter and wavelength. Interestingly, the induced jitter scales reasonably well with the Rytov number. This linear fit is used in the system engineering analysis. Figure 6 shows the result; Holmes' figure is shown with the linear fit overlay:

$$\sigma_{\text{Sct}} = T_F \cdot \frac{1.32 \cdot \text{Rytov}}{\sqrt{2}} \frac{\lambda}{D_R}$$

$$= 0.933 \cdot T_F \cdot \text{Rytov} \frac{\lambda}{D_R}. \tag{32}$$

The $1.32 \cdot \text{Rytov}$ comes from Holmes's[6] work (with the diffraction λ/D_R term). The $\sqrt{2}$ is required to convert from his two-axis numbers to the single-axis numbers used here. The T_F represents the filtering attenuation of the track control loop. Note that the scaling factor 0.933 was derived for one particular propagation path. An investigation is required to determine how much this parameter might vary from one application case to another.

Table 3. Parameter values used for jitter budget calculations

Parameter	Units	G-S Value	Comments
Lambda - λ	μm	1.06	Illuminator Wavelength
Receiver Aperture - D_R	m	3.5	Receiver Aperture Diameter
Tracker SNR	–	7	
Track Filter Factor	–	0.4	
Fried Coherence Parameter r_0	cm	12	At wavelength over the propagation path; scenario and atmosphere dependent
AO Array Size, n	–	15	
Tracker Detector IFOV	nrad	1000	
Diameter PSF - D_{SPF}	μrad	285	
Target/ Algorithm Factor χ_{TA}	–	1	
Tyler Frequency - f_{TG}	Hz	14	scenario and atmosphere dependent
Tracker 3dB Bandwidth - f_{3dB}	Hz	100	
Tracker Bandwidth - f_{BW}	Hz	100	Defined here as the open loop gain crossover. For 1st order track systems $f_{BW}=f_{3dB}$
Local Mount Jitter rms Tilt - σ_{MJ}	μrad	0.15	
Mount Jitter Effective Bandwidth - f_d	Hz	50	
Uplink Jitter rms Tilt - σ_T	μrad	3	
Illumination Diameter (at Target) D_I	μrad	15	
Target Angular Diameter - D_T	μrad	4	Variable; One Case Selected Here
Number of Illum Beamlets - N_B	-	1	
Rytov Parameter - Rytov	-	0.05	scenario and atmosphere dependent
Scintillation Factor χ_{Sct}	–	1.32	See Analysis based on Holmes Paper
Track Normalization Factor - K_{Tkr}	–	0.25	For alternative track measurement noise formulation

Based on this result, either a single value or a table of values would be required for a general system engineering result.

3. Application Example: Generic Ground-to-Space Imaging Application

A numerical error budget example was generated for active track systems representative of those used in a generic ground-to-space imaging application. The parameter values used in the error budget analysis are shown in Table 3. Calculated values derived from these parameters are given in Table 4.

These parameter values were applied to calculate a track jitter error budget. Figure 7 shows the result for the Tyler and Fried track noise result for the assumed 3-μrad target size (1.2 m at 400-km range). The chart shows the individual error contributions for the contributors: (1) track jitter (track sensor noise), (2) residual atmospherics tilt jitter, (3) residual local disturbance jitter, (4) jitter coupling, and (5) active signature jitter. The chart also shows (upper right) the net LOS jitter of an "equivalent" passive track system. We have defined an "equivalent" passive track system to be one in which the track noise contribution is the same as that of the active system. This is the same as assuming that the SNR and wavelengths are the same. Then the equivalent total tracking jitter is obtained by just RSSing the first three terms (i.e., excluding the jitter coupling and active signature terms).

Table 4. Calculated values used for jitter budget calculations

Calculated Values	Units	G-S Value	Comments
Normalized Target Size- nT	–	13	Measured in Units of Diffraction Spots
SNR Factor χ_{SNR}	–	0.75	Function of SNR; SNR of 7 Assumed for SOR
AO Factor χ_{AO}	–	1.94	Tracker Noise Degradation Factor for Atmospheric Turbulence Effects and an Imperfect Adaptive Optics Correction System. This is a calculated parameter dependent upon the turbulence characterization parameters R (Rytov) and r_0 (Fried parameter) and the re
FPA Sample Factor χ_{FPA}	–	1.00	
Jitter Couple Factor - χ_{JC}	–	0.1	Calculated from fit to analytic data in Riker paper. {See Jitter Couple Factor Spreadsheet for details]
Diffraction Sot Size λ/D	μrad	0.303	

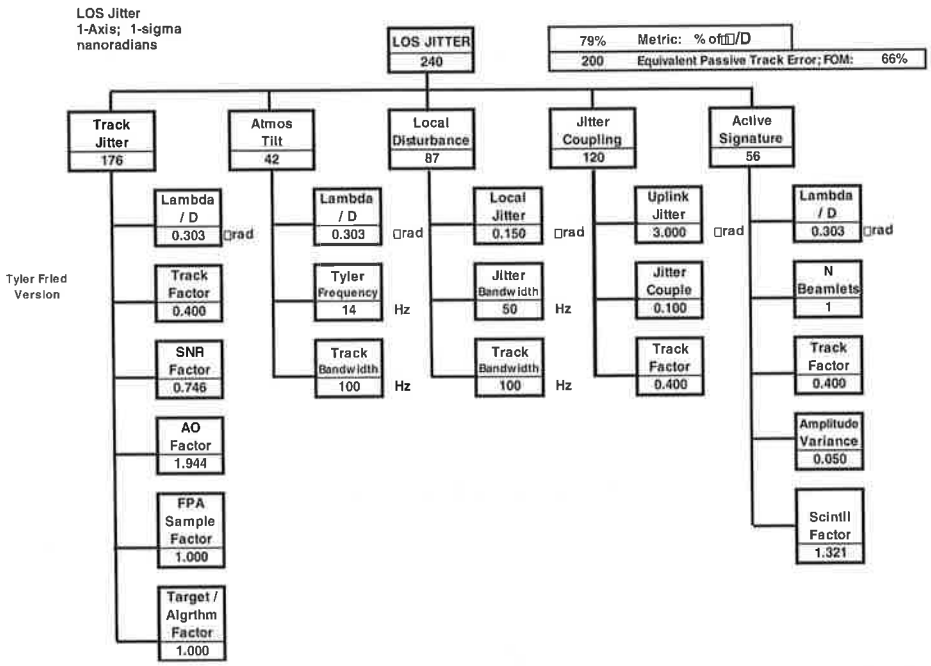

Fig. 7. Active track error budget example for a ground-to-space imaging application example system: Tyler and fried track measurement error model [Eq. (2))]: (SNR = 7; $n_T = \sim 13$).

Some interesting observations can be made from examination of these LOS jitter performance error budgets:

- Track sensor measurement jitter is the dominant term.
- Jitter coupling is the second dominant term.
- Atmospheric tilt and active signature residuals are relatively negligible contributors.
- Net error is >3/4 λ/D, substantially larger than a typical design goal of 1/4 λ/D.

– An "equivalent" passive track system (i.e., one with no jitter coupling or active signature errors) has 17% improved track error or ~0.66 λ/D (which equates to a 20% penalty for active track versus passive track for this example).

The jitter coupling is nearly as large as the track measurement noise. Although at first this result might appear surprising, note that (1) uplink jitter may be several times larger than receiver LOS jitter, due to the transmitter's small aperture; (2) illuminator beams are designed to be larger than the target (3–4× larger) so as to maintain SNR at limited power, with the consequence that the jitter coupling factor is at least 10%. These terms combine to give jitter coupling errors that are a relatively large fraction of the receiver jitter.

4. Design Synthesis

The system engineering error budget supports the following design synthesis procedure:

– For a shared aperture tracking/imaging system, choose λ/D as required to support imaging resolution of HEL beam projection requirements.
– Select a nominal SNR (~7) recognizing that higher ratios will place stringent demands on illuminator power and engagement range. (Select larger SNR values if design margin is desired.)
– Specify required adaptive optics performance (<2× diffraction limit) for the portion of the adaptive optics that impacts the tracking system. (Higher Strehl ratios are needed for the HEL projection system.)
– Specify control bandwidth (sufficiently large that residual atmospheric and local disturbance jitter are less than track measurement noise jitter).
– Design local jitter amelioration and control as smaller than track measurement noise jitter (couples with the bandwidth trade).
– Determine corresponding second-tier parameters (i.e., SNR → illuminator power and beam quality, transmit aperture, target cross section and detector noise).
– Investigate design with more detailed models.

5. Acknowledgment

This work was sponsored by the Air Force Research Laboratory Directed Energy Directorate (AFRL/RDKB) under contract FA9451-07-C-0205.

References

[1]Andrews, L. C., *Field Guide to Atmospheric Optics*, SPIE Field Guides, Volume FG02, SPIE Press, Bellingham, WA (2004).

[2]Andrews, L. C., and R. L. Phillips, *Laser Beam Propagation through Random Media*, 2nd ed., SPIE Press, Bellingham, WA (2005).

[3]Baribeau, R., and M. Rioux, Appl. Opt. **30**(26), 3752 (1991).

[4]Brunson, R.L., J. F., Riker, and G. A. Crockett, "Overview of Acquisition, Tracking, and Pointing (ATP) and Fire Control (FC) Algorithms Using a Simulation (TASAT)," AIAA Fire Control Conference, 8–10 July 1992.

[5]Fugate, R. Q., *Adaptive Optics*, Chapter 5, Part 2 of. Vol 5, *Handbook of Optics*, 3rd ed., Optical Society of America, McGraw Hill, New York, NY (2009).

[6]Holmes, R., J. Opt. Soc. Am. A **26**(2), 313 (2009).

[7]Jelalian, A. V., *Laser Radar Systems*, Eq. 1.2, Artech House, Norwood, MA (1992).

[8]Riker, J. F., "Laser Requirements for Active Tracking at SOR," Diode Laser Technology Review (DLTR), Albuquerque, NM, (1997).

[9]Sher, L. *Centroid Jitter Due to Speckle* (Unpublished technical note obtained from the author), October 8, 2001.

[10]Tyler, G., and D. Fried, J. Opt. Soc. Am. A **72**(6) 804 (1982).

The Authors

Mr. Richard L. (Dick) Brunson retired from the Air Force in 1987, having served in a career that included assignments as an intelligence specialist in Viet Nam, flight test engineer, and R&D positions including the Air Force Weapons Laboratory (AFWL). During his AFWL assignment he served as an Air Force Division Chief at the Starfire Optical Range (SOR) during the early days of classified atmospheric compensation programs in the 1980s. Since then, he led and technically contributed to optical system modeling, simulation, system analysis, control system design, and estimation efforts at RDA, Aerospace Corporation, SVS, and Boeing-SVS until his retirement in 2010.

Dr. David R. Dean has been a key technical contributor throughout his career on state-of-the-art development of high-energy lasers, beam control systems, and surveillance and tracking sensor systems. Dr. Dean was instrumental in the development of the tri-service gas dynamic laser while at the Air Force Weapons Laboratory (now the Air Force Research Laboratory). During his career he has also worked at Perkin-Elmer, Hughes Danbury Optical Systems, Hughes, Raytheon, and Boeing-SVS. His recent interests have included adaptive optics, 3-D photon counting lasers, and IR sensor systems.

Mr. Edward A. Duff's career has been with the US Air Force, first as a career officer (USAF Colonel, Retired) and then as a civil servant. Ed has specialized in directed energy (DE) system beam control, pointing and tracking, and DE applications. He has extensive experience with electro-optical trackers, track algorithms, and DE system analysis. Currently he is an Air Force civilian employee (DR-IV, DAF), an AFRL Fellow, and the Long Range Strike Product Line Leader at the Directed Energy Directorate (AFRL/RDTP) Air Force Research Laboratory.

Dr. Joshua L. Kann has a Ph.D. in Optical Sciences from the University of Arizona. From 1992 to 1999 he worked as a research scientist with the Air Force Research Laboratory (AFRL), first in the Sensors Directorate and then in the Directed Energy Directory. Since 1999 Dr. Kann has worked with SVS, Boeing-SVS, and Boeing-LTS. He now works at Boeing/DES performing technical support to the Air Force Starfire Optical Range. For the past 15 years he has been working in the field of directed energy systems, with an emphasis on active track and active imaging systems. He has been involved in both design and analysis of these systems as well as integration and testing.

Dr. James E. Negro has many years of experience in design engineering, project management, and technical staff management for high-technology aerospace organizations, having worked for the Air Force, the Draper Laboratory, and Boeing-SVS. He currently works as a Technical Fellow at Boeing-SVS. His technical work has emphasized the design, analysis, evaluation, development, and testing of airborne and space-based precision electro-optical systems for specializing in high-energy laser pointing and imaging applications. He has also worked on precision vehicle control, autonomous control, and navigation system applications. His expertise includes servo control design for precision optical alignment, beam control and tracking systems, and analysis and performance evaluation of precision navigation systems, including attitude knowledge.